THE MICROSTRUCTURE OF LUNAR MICROMETEORITE IMPACT CRATERS. S. K. Noble[1] L. P. Keller[2], R. Christoffersen[2,3] and Z. Rahman[2,3], [1]NASA Headquarters, 300 E St SW Mail Code 3D75, Washington DC 20546, sarah.k.noble@nasa.gov, [2]NASA JSC, Houston TX 77058, [3]Jacobs Technology Inc, Houston TX.

Introduction: The peak of the mass flux of impactors striking the lunar surface is made up of objects ~200 μm in diameter that erode rocks, comminute regolith grains, and produce agglutinates. The effects of these micro-scale impacts are still not fully understood. Much effort has focused on evaluating the physical and optical effects of micrometeorite impacts on lunar and meteoritic material using pulsed lasers [e.g. 1, 2, 3] to simulate the energy deposited into a substrate in a typical hypervelocity impact. Here we characterize the physical and chemical changes that accompany *natural* micrometeorite impacts into lunar rocks with long surface exposure to the space environment (12075 and 76015). Transmission electron microscope (TEM) observations were obtained from cross-sections of ~10-20 μm diameter craters that revealed important microstructural details of micrometeorite impact processes, including the creation of npFe^0 in the melt, and extensive deformation around the impact site.

Samples: Lunar rock 76015 is a noritic breccia coated with a thick patina, which we have previously described [4, 5, 6]. The cosmic ray exposure age is well constrained at 22 My [7, 8]. Lunar rock 12075 is an olivine basalt with large olivine phenocrysts (1-2 mm). The surface contains numerous micrometeorite impact craters ranging from 100 μm down to 1 μm. The solar flare track density in olivine (~10^{11}/cm^2) indicates a minimum surface exposure of ~10^6-10^7 years.

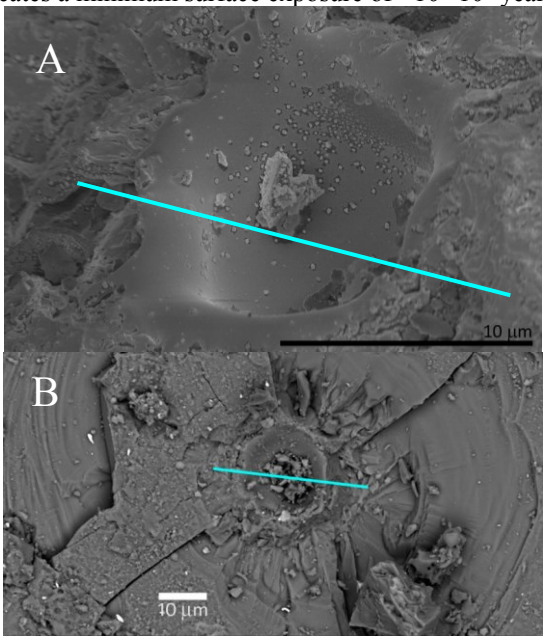

Fig 1. Impacts into plagioclase (A) and olivine (B). The approximate location of the FIB samples are indicated in blue.

Methods: Small chips of the rocks were examined by SEM to locate an impact crater into plagioclase (76015) and olivine (12075) of appropriate sizes for FIB sectioning and analytical TEM characterization. The plagioclase impact is about 10 μm in diameter, the olivine impact is around 18 μm (fig 1).

Results:

Plagioclase: The crater is lined with a ~1 μm thick glass layer, compositionally indistinguishable from the host plagioclase (fig 2). The melt layer is slightly thicker at the bottom than the sides. The melt transitions into a narrow shocked region with numerous defects and dislocations (fig. 3), which extends ~0.5-1 μm beyond the melt zone. Radial fractures are readily apparent surrounding the crater.

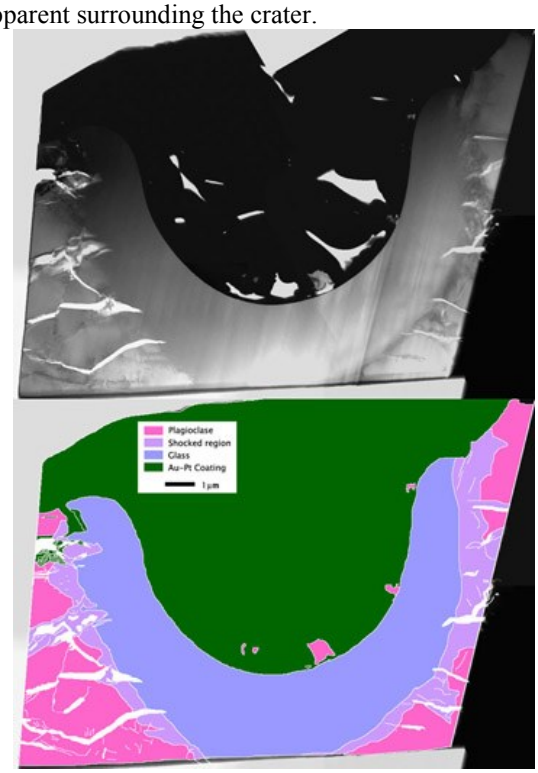

Fig 2. TEM bright field image (top) and corresponding map of the plagioclase impact.

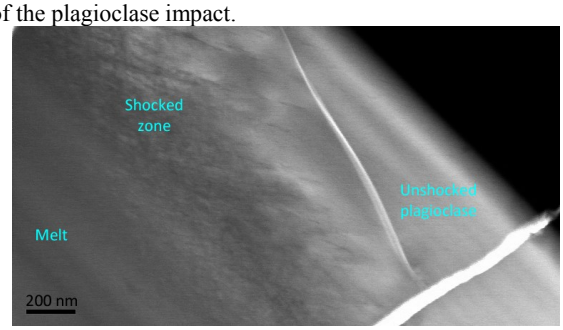

Fig 3. TEM bright field image of shocked zone.

Olivine: Extending from the crater cavity outward into the host olivine grain, the crater walls are composed of a shock-melted lining, ~0.5–2 µm thick, of glassy olivine with the same composition as the unmelted grain. (fig 4). The melt layer sharply transitions to an underlying layer of polycrystalline olivine that appears to have recrystallized upon cooling (fig 5). The recrystallized olivine becomes progressively finer-grained as it transitions to the underlying olivine single-crystal.

An extensive zone of shocked and deformed olivine, containing radial fractures and numerous defects and dislocations, extends outward 15-20 µm from the melt recrystallized zone. The shock effects here extend much further from the crater center than we observe with plagioclase. Unshocked areas of the host olivine contain a high density of solar flare particle tracks (~10^{11}/cm^2), but closer to the crater, the tracks are annealed.

NpFe^0 is present throughout the melt and recrystallized layer (fig 5); it is remarkably consistent in size (~3-7 nm dia.). The upper ~70 nm is vesiculated, likely the result of implanted solar wind gases, and the top surface is highly enriched in npFe^0 and may represent a vapor-deposit.

Discussion: The two impacts share much in common in term of their basic structure of melt lining/shock zone/radial fracturing. However, the shock zone is much more extensive in the olivine and there is no evidence of recrystallization in the plagioclase or annealing of solar flare tracks.

The olivine sample clearly demonstrates that a natural micrometeorite impact into a Fe-bearing olivine single-crystal can produce an olivine-composition shock melt glass that is mostly un-devitrified except for the presence of abundant npFe^0 inclusions. It does not, unfortunately, inform us whether solar wind H^+ is required in the impacted surface for npFe^0 formation, since most exposed lunar surfaces are saturated with solar wind ions [9]. The size distribution and narrow range of the npFe^0 is mostly similar to that in grain rims rather than the much larger sizes and wider size range observed in agglutinitic glasses. This suggests that sequential impact processing is required for npFe^0 to coarsen to the sizes seen in lunar agglutinitic glass.

While pulsed-laser experiments produce glassy olivine containing npFe^0, they fail to produce the deformation effects (shock vitrification, dislocations, fracturing) that are observed in the natural impact craters.

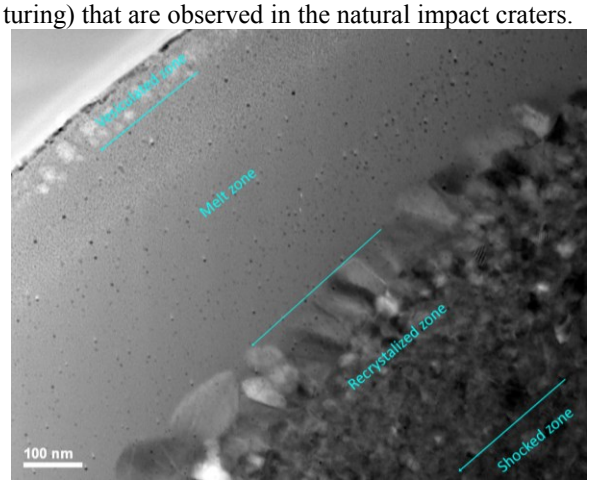

Fig 5. TEM bright field image of the impact melt lining.

Future work: Future work will focus on analyzing additional craters in olivine as well as other phenocrysts in the 12075 (e,g, pyx and ilm) and comparing the results to laboratory impact experiments.

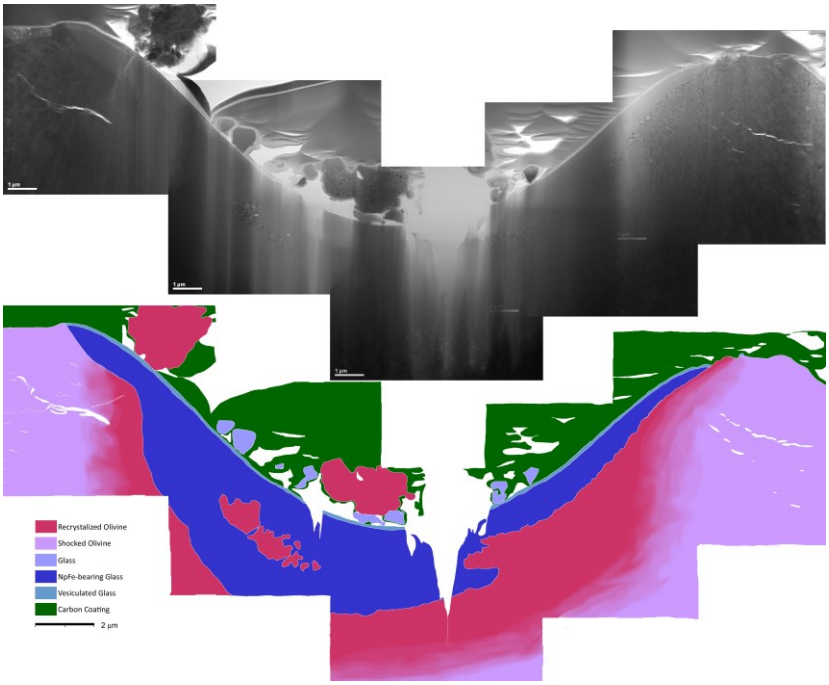

Fig 4. TEM bright field image (top) and corresponding map of the olivine impact.

References: [1] Sasaki et al. (2001) *Nature, 410,* 555-557. [2] Brunetto R. et al. (2006) *Icarus, 180,* 546-554. [3] Loeffler et al. (2009) *JGR, 114* EO3003. [4] Noble S. K., et al. (2007) *LPSC38,* Ab #1359. [5] Noble S. K., et al. (2012) *LPSC43 Ab #1239*. [6] Noble S. K., et al. (2013) *LPSC44* Ab #1298. [7] Crozaz et al. (1974) 5th *PLPSC,* 2475-2499. [8] Arvidson et al. (1975) *Earth, Moon, and Planets, Vol 13, 259-276.* [9] Borg et al. (1980) *Proc. Conf. Ancient Sun*, 431-461.